Optical Pumping of Rubidium Vapor

Emily P. Wang
MIT Department of Physics

The technique of optical pumping is used to measure how the characteristic pumping time τ of Rb varies according to the temperature and intensity of the beam of irradiating photons. We found that τ decreased with increased beam intensity and increased with increased temperature. This agrees with physical intuition, but our mathematical model for the effects of temperature must be reconsidered. By slowly varying $\vec{B}$, we obtain the $|\vec{B}| = (294.1\pm21.1)$ mgauss for the Earth's ambient field, which is correct to an order of magnitude. We also obtain 1.49 ± 0.01 for the ratio of the Landé g factors for the ground states of Rb^{87} and Rb^{85}, which compares well to the theoretical value of 1.5. For the magnitudes of the values of the Landé g factors, we obtain $g_f(Rb^{87}) = .520 \pm .001$ and $g_f(Rb^{85}) = .319 \pm .001$, while the theoretical values are $g_f(Rb^{85}) = \frac{1}{3}$ and $g_f(Rb^{87}) = \frac{1}{2}$.

1. INTRODUCTION

Optical pumping is a process of raising individual atoms from lower to higher states of internal energy—this process is used to alter the equilibrium populations of atoms in different energy levels to prepare them for spectroscopy. The word "optical" refers to the light energy that powers this atomic pump. The motivation for pumping atoms is to prepare them for a particular kind of spectroscopic analysis. Atoms can emit and absorbe electromagnetic radiation varying from radio waves, whose wavelengths are on the order of hundreds of meters, to X-rays, which are a thousand times shorter than visible light waves. By the 1960s, the visible and X-ray spectra of atoms had been extensively researched, but exploration of the radio-frequency region of atomic spectra had only begun [1].

In the 1940s, microwave and radiofrequency spectroscopy was used to determine atomic and molecular structure–nuclear spins and moments in particular. In 1949, Bitter raised the possibility of detecting radiofrequency resonances through optical means [2]. In 1966, A. Kastler realized this possibility with the invention of called optical pumping, a new way of doing radio-wave spectroscopy. The g-factor and the lifetime of excited states could be determined from such experiments. Practical applications of optical pumping include the maser, the laser, and very sensitive magnetometers. In 1957, Dehmelt introduced the transmission technique of detecting magnetic resonances in the ground state of alkali metal vapors [2], a method that we make use of in this experiment.

2. THEORY

2.1. Optical Pumping of Rubidium Vapor

We investigated the radio-frequency transitions in Rb^{87} and Rb^{85}. Rubidium is an alkali metal atom that has a $^2S_{1/2}$ ground state and $^2P_{1/2}$ and $^2P_{3/2}$ excited states (Figure 1). The optical transitions between the ground state and the two excited states are the origin of the D_1
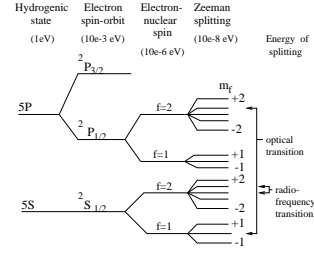

FIG. 1: Adapted from [3]

and D_2 lines, respectively. In our experiment, the D_2 line is removed from the light source by means of an narrow band filter—we are only concerned with exciting the transition between the $^2S_{1/2}$ state and the $^2P_{1/2}$ state. Both the difficulty and the great effectiveness of using radio waves in atomic spectroscopy is due to the low energy of radio waves. When atoms absorb or emit radio waves, they experience a slight change in their magnetic energy. These transitions in energy states can happen spontaneously in either direction–atoms at higher levels will fall into the lower level, and those in the lower level will jump to the higher one, provided that the necessary quanta of energy is available. For transitions to be detected in a sample of matter, there must be an overall excess of upward or downward jumps in energy among a population of atoms [1].

At equilibrium, the atomic populations of two energy levels, n_1 and n_2, is given by the Boltzmann Distribution: $\frac{n_1}{n_2} = e^{-\frac{\Delta E}{kT}}$ where ΔE is the energy difference between the two levels, k is Boltzmann's constant, and T is temperature. For the radiofrequency transitions we wish to observe, ΔE is 10^{-8} eV at room temperature, kT is 0.25 eV, and $\frac{n_1}{n_2}$ differs from unity by only one part in 10^6, and transitions between the two levels are very difficult to observe.

Here optical pumping comes into play, altering the populations of the energy levels in such way that the atomic transitions can be detected with more ease. Figure 2 illustrates the general principle of optical pumping. We look at three levels: A, B, and C, two of which are closely spaced together. The transitions A↔C and B↔C
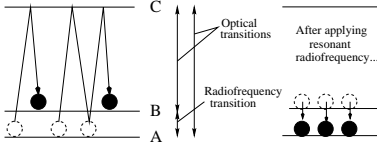
FIG. 2: Adapted from [1]. Shown are the results of optical pumping and the subsequent application of a radio-frequency signal that destroys the pumped state.

are accompanied by the absorption or emission of an optical photon, while the transition A↔B is accompanied by the absorption or emission of a photon of radiofrequency. Before optical pumping begins, atoms are located in the lower two energy levels with an almost equal probability[1].

When a lamp emitting optical photons is shined onto atoms in a vapor, the photons excite atoms in level A to level C, where they remain momentarily before falling back to either B or A. If the atoms drop back to A, they may be excited again, but if they drop back to B, there they will remain, for they may no longer absorb photons of optical wavelength. As time passes, the net effect is to "pump" atoms from level A to level B. This state can be detected by observing the transmitted light that passes through the vapor of atoms, such as with a photodiode detector. When all of the atoms have been pumped up to the B level, they are no longer able to absorb incoming radiation, and the vapor is relatively transparent to the lamp's light.

The pumped state can be destroyed by applying a radiofrequency that equals the resonant frequency of the atom–namely, the frequency corresponding to the transition between levels A and B. This change in situation, too, can be observed by measuring the transmitted light. A sudden increase in opacity would indicate that the pumped state has been destroyed, and the atoms which drop back down to level A are once again able to absorb incoming radiation. Optical pumping can be used to measure the relaxation times of magnetic moments of atoms, the magnetic field experienced by the atoms, and the Landé g factors of atoms.

2.2. Zeeman Effect, Derivation of Landé g factor

The Landé g factor is a dimensionless factor which corrects for the magnetic interactions in the atom that alter an atom's energetic states. When an atom is placed in a uniform external magnetic field B, the energy levels will be shifted, and this phenomenon is called the Zeeman effect. Following the analysis in [4] and [5], for a single electron, the perturbation of the energy levels is given by

$$H'_z = -(\vec{\mu_l} + \vec{\mu_s})\vec{B} = \frac{e}{2m}(\vec{L} + 2\vec{S})\vec{B} = -\vec{\mu_J}\vec{B} \quad (1)$$

where $\vec{L}$ is the orbital angular momentum operator, $\vec{S}$ is the spin operator, μ_l is the dipole moment associated with orbital motion μ_s. μ_j, the combined magnetic moment, is given by $\mu_j = -g_J\frac{e}{2m}\vec{J}$, where g_J is the Landé g factor of interest, which we will now seek to calculate.

When the strength of the external magnetic field experienced by the atom is much greater than the strength of the internal field, then the fine structure dominates, and H'_z can be treated as a small perturbation. This is called the weak-field Zeeman effect, and is the regime of Zeeman splitting that we are concerned with in this experiment. The magnitude of splitting is given by $E'_z = \frac{e}{2m}\vec{B} < \vec{L} + 2\vec{S} >$. When the fine structure dominates, we can use the basis $|n, l, j, m_j >$, where n is the principle quantum number, l is the quantum number associated with $\vec{L}$,, j is the sum of the spin (given by the quantum number s) and l, and m_j is a quantum number that takes on values from $|l - s|$ to $l + s$. We use this basis because $\vec{S}$ and $\vec{L}$ are not separately conserved in the presence of spin-orbit coupling. Using the vector model, we see that $\vec{J} = \vec{L} + \vec{S}$ remains constant, and $\vec{L}$ and $\vec{S}$ precess quickly around this fixed vector sum. Using the fact that the time average value of $\vec{S}$ is its projection along $\vec{J}$, we can obtain the value of $< \vec{L} + 2\vec{S} >= g_J\vec{J}$, giving us the g factor we desire:

$$g_J = 1 + \frac{j(j+1) + s(s+1) - l(l+1)}{2j(j+1)} \quad (2)$$

To further correct the energies of the system, we take into account the fact that the nucleus of the atom also has an angular momentum, given by the operator $\vec{I}$ and the quantum number i. The total angular momentum of the atom is now described by $\vec{F} = \vec{J} + \vec{I}$, and the dipole moment of the atom is now given by the equation $\vec{\mu} = g_f\frac{e}{2m}\vec{F}$, where g_f is the new Landé g factor we must calculate.

Using a similar procedure to the one used to calculate g_J, we note that $\vec{J}$ and $\vec{I}$ now precess around their sum $\vec{F}$. Because the nucleus is so massive, however, it has a much smaller angular momentum than electrons, so the Landé g factor associated with $\vec{I}$, g_I, is negligible, and the precession of $\vec{I}$ around $\vec{F}$ can be ignored in the analysis [5]. Carrying through with the algebra once more, we obtain

$$g_f = g_J[\frac{f(f+1) + j(j+1) - i(i+1)}{2f(f+1)}] \quad (3)$$

where g_J was derived above. Evaluating these theoretical expressions for the ground state of the two different rubidium isotopes used in this experiment, we find that both isotopes have $g_J = 2$, $g_f(Rb^{85}) = \frac{1}{3}$, and $g_f(Rb^{87}) = \frac{1}{2}$.

2.3. Characteristic Time Constant τ for Optical Pumping

Our physical intuition tells us that increasing the rate of orientation, such as by increase the light intensity, we

should expect a decrease in the time it takes for atoms to become optically pumped, and hence there should be a decrease in the time constant. If we increase the rate of disorientation, such as by increasing the collisions of atoms with each other by increasing the temperature, we should increase the pumping time constant. The mathematical model is $\tau = \frac{1}{W_u + W_d}$, where W_u is the rate of transitions to the pumped state and W_d is the rate of transitions out of the pumped state.

3. EXPERIMENT

In this experiment, we used circularly polarized light from a rubidium lamp to irradiate rubidium vapor to excite the optical $^2S_{1/2}$ state to $^2P_{1/2}$ state transition (the D_1 line, as mentioned above). Every photon has angular momentum $\pm\hbar$, so transitions in the Rb atoms will have $\Delta m_f = 1$. Spontaneous transitions can occur with $\Delta m_f = \pm 1, 0$. As a result, there will be a net pumping of atoms to the $m_f = +1$ substate of the lower electronic state, for once atoms land there, they are unable to absorb another circularly polarized photon.

3.1. Slowly Varying $\vec{B}$

The setup used in this part of the experiment is shown in Figure 3. The rubidium lamp was first heated to a temperature of approximately 40 degrees Celcius, and the beam of light was focused by two lenses so that it hit the photodiode squarely in the center. The photodiode observed the amount of light that traversed the cell of Rb vapor located in the center of the apparatus, and its output was input to the oscilloscope. A relatively high transmittance was observed once the state of pumping had been achieved, and when a sudden dip in transmittance was observed (sudden increase in vapor opacity) it could be deduced that a resonant radiofrequency had been reached and the pumping state had been temporarily destroyed.

To measure the ambient $\vec{B}$ of the Earth, as well as the ratio and the values of the g factors for Rb, a radiofrequency sweep was performed by hooking up the function generator to the RF coils surrounding the Rb vapor cell, and the $\vec{B}$ external to the atom was slowly varied. We note that the resonant frequency f of rubidium is related to the magnetic field experienced by the atom, $\vec{B}$, in the following way: $f = \frac{g_F \mu_B \vec{B}}{h}$, and that $\vec{B}$ will have three components: $|\vec{B}| = \sqrt{B_x^2 + B_y^2 + B_z^2}$. Our goal was to produce a magnetic field that just canceled out the Earth's $\vec{B}$ and thereby minimized the resonant frequency observed in the Rb atoms. This was accomplished by varying first the B_x until the resonant frequency had been minimized, re-setting B_x to this value, and repeating the procedure with the B_y and the B_z in
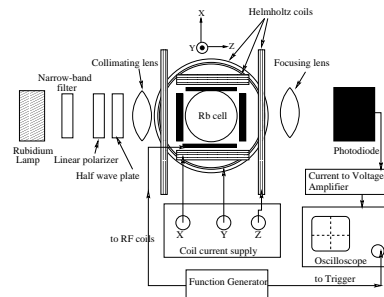

FIG. 3: Setup for optical pumping, showing coordinate system used—setup used to vary the $\vec{B}$ in order to obtain ambient field magnitude and ratio and values of Landé g factors.

the Helmholtz coils. The $\vec{B}$ obtained at that time was the $\vec{B}$ needed to cancel out the Earth's $\vec{B}$, and therefore was equal in magnitude to the Earth's $\vec{B}$. The value of the resonant frequency was measured by using the cursors on the oscilloscope screen to obtain the location of the absorption peaks that indicated the disturbance of the pumped vapor state.

To produce and vary the magnetic field external to the atom in the x-, y-, and z-directions as desired, three sets of Helmholtz coils were placed around the Rb vapor cell, and current was run through these coils, as shown in Figure 3. Helmholtz coils consist of pairs of identical coils which are spaced at a distance equal to their radii. They produce a magnetic field at a point directly between the centers of each coil which is given by $\vec{B}_{HC} = \frac{8\mu_0 N \vec{I}}{\sqrt{125}R}$, where $\vec{I}$ is the current in the Helmholtz coil, R is the radius of the coil, N is the number of turns in the coil, and μ_0 is an SI constant equal to $4\pi \times 10^{-7}$ Wb A^{-1} m^{-1}. If we substitute this into the equation for the resonant frequency of the Rb atoms, we obtain the following equation:

$$
\begin{aligned}
f &= \frac{g_F \mu_B}{h} \sqrt{B_x^2 + B_y^2 + B_z^2} \\
&= \frac{g_F \mu_B}{h} \frac{8\mu_0}{\sqrt{125}} \sqrt{(\frac{N_x \vec{I_x}}{R_x})^2 + (\frac{N_y \vec{I_y}}{R_y})^2 + (\frac{N_z \vec{I_z}}{R_z})^2}
\end{aligned}
\quad (4)
$$

From Equation (4), we can see that the characteristics of the frequency for varying I_x and I_y will be hyperbolic. Once B_x and B_y are set to equal zero, however, the characteristic of the frequency for the varying of I_z will simply be symmetrically linear.

3.2. Characteristic Time for Optical Pumping

In this part of the experiment, we first bucked out the vertical and lateral components of the Earth's magnetic field using the x and y Helmholtz coils, using the values obtained previously. The z-coil's current was then turned on and off using the square wave on a second function generator hooked up to the current controls. The waveforms which showed the change in opacity as a function

of time after turning on and off the current were captured on the oscilloscope and later analyzed to obtain the values of the time constant τ related to the optical pumping of the system.

The pumping rate was varied by changing the intensity of the incoming light beam from the Rb lamp. Filters of optical density 0.1 were used to progressively block out more and more light, and a screen capture of the changing opacity was taken at each level of filtering, up to five filters. The density of the Rb vapor was also altered by changing the temperature of the bulb.

4. RESULTS AND ERROR ANALYSIS

4.1. Measurement of the Ambient $|\vec{B}|$, Landé g factors

Following Equation (4), the fit line used for I_x and I_y was hyperbolic: $y = \frac{b}{a}\sqrt{c^2 + (x - x_0)^2} + d$. The fit line used for I_x was linear, consisting of one line of negative slope and one line of postive slope. The values of I_x and I_y at the minimum resonant frequency were obtained from the fit parameter x_0. The two lines were fitted separately, and the value of I_z at the point of intersection was noted. Note each graph shows a plot for both Rb^{87} and Rb^{85}. To obtain final values for current values in each direction that minimized the resonant frequency (and therefore produced the correct $|\vec{B}|$ to cancel out the Earth's field), the current values obtained from the fits for each isotope were averaged, and errors were added in quadrature. The current values are shown on the plots in Figures 4 and 5.

In the I_z plots, the z-intercept for each isotope was calculated with the following equation: $I_z = \frac{a_{r1} - a_{l1}}{a_{l2} - a_{r2}}$, where a_{r1} and a_{r2} were the y-intercept and slope, respectively, of the line on the right, while a_{l1} and a_{l2} were the y-intercept and slope of the line on the left. The error was calculated with the following equation: $\sigma_{I_z} = \sqrt{I_z[\frac{\sigma_{r1}^2 + \sigma_{l1}^2}{(a_{r1} - a_{l1})^2} + \frac{\sigma_{l2}^2 + \sigma_{r2}^2}{(a_{l2} - a_{r2})^2}]}$, where the error in each fit parameter was obtained from the fitting script. The error for each datapoint, which was input into the fitting script, was obtained by noting the resolution of the cursor used to measure the location of the resonant peaks. Unfortunately, we were unable to fit the peaks to curves due to a difficulty in the osciloscope-to-computer capture program.

The values for the current in each direction were then substituted into the equation for the $\vec{B}$ created by Helmholtz coils was then used to calculate the components of the $\vec{B}$ necessary to cancel out Earth's $\vec{B}$. The error in each component of the magnetic field was calculated by error propogation based on the equation for the magnetic field of a Helmholtz coil, given the current, number of coils, and radius characterizing the Helmholtz coil: $\sigma_B = \sqrt{B^2(\frac{\sigma_I^2}{I^2} + \frac{\sigma_R^2}{R^2})}$. The value obtained for the Earth's magnetic field using this method
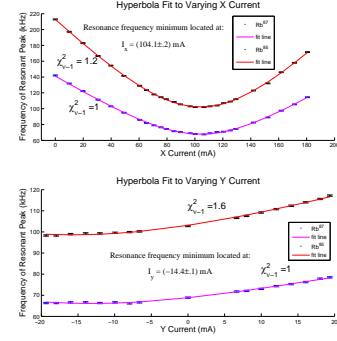

FIG. 4: Varying x- and y-current and observing change in resonant frequency of the two Rb isotopes.
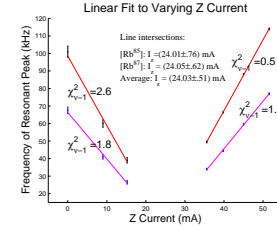

FIG. 5: Varying z-current and observing change in resonant frequency of the two Rb isotopes. Note that the errorbars are larger for the lines on the left, as it was more difficult to make out the location of the resonant frequency peaks for those points.

was (294.1 ± 21.1) mgauss, compared to the ≈ 300 mgauss measured using a magnetometer in the lab, and the actual value of the $\vec{B}$ at our longitude and latitude, which is ≈ 600 mgauss. The reason for this discrepency between measurement and accepted value is likely due to the presence of a large metal pipe directly above the experimental setup, which caused the magnetic field in the room to be distorted.

As the resonant frequency of each isotope is directly proportional to its g factor, the ratio between the g factors of Rb^{87} and Rb^{85} was obtained by taking all the values for the resonant frequencies of Rb^{87} and dividing by all of the resonant frequencies of Rb^{85}. The ratio obtained in this fashion was 1.49 ± 0.01. Error was obtained by adding in quadrature the standard deviations of the resonant frequencies of Rb^{87} to the standard deviations of the resonant frequencies of Rb^{85}.

To obtain the actual values of the Landé g factors, Eq. (4) was again used to determine how the g factors were related to the parameters obtained in the fitting of the resonant frequency vs. current plots. Error was propagated using the errors obtained for the parameters through the fitting program that, again, had been input with errors for each datapoint relating to the resolution of the oscilloscope cursor. The values of the Landé g factors obtained were $g_f(Rb^{87}) = .520 \pm .001$ and $g_f(Rb^{85}) = .319 \pm .001$, while the theoretical values are $g_f(Rb^{85}) = \frac{1}{3}$
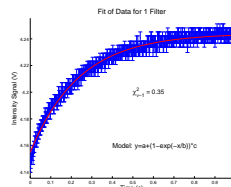
FIG. 6: A sample of the data taken for the portion of this experiment involving the measurement of the time constant for rubidium pumping.
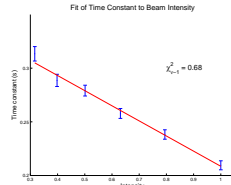

FIG. 7: Varying the beam intensity and observing its effect on the time constant.

and $g_f(Rb^{87}) = \frac{1}{2}$.

4.2. Characteristic Time for Optical Pumping

A portion of a typical screen capture from the oscilloscope is shown in Figure 6. All data taken in this part of the experiment were fitted to exponential curves, which allowed determination of the time constant that characterized the optical pumping process. To obtain error on the exponential fits, error for each individual datapoint was estimated as a percentage of the signal, with additional error from deviations in temperature and determining the time of the polarity flip. The observed dependence of the time constant on the temperature and beam intensity were then compared to our physical intuition and our mathematical models. We observed that the time constant decreased with a increase in beam intensity, as expected from both physical intuition and mathematical models, but that the time constant increased with an increased temperature, agreeing with the physical intuition but not the mathematical model.
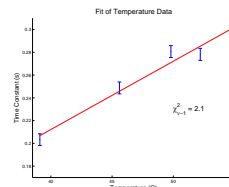

FIG. 8: Varying of temperature and observing its effect on the time constant.

5. CONCLUSIONS

We found that τ decreased with increased beam intensity and increased with increased temperature, agreeing with physical intuition on both counts, but disagreeing with our mathematical model for the effects of temperature, suggesting we should reconsider our model. Other improvements would be to more accurately control the temperature during the temperature-varying trials. We obtained that the Earth's ambient magnetic field has a magnitude of $|\vec{B}| = (294.1 \pm 21.1)$ mgauss, which is correct to an order of magnitude, but is inaccurate due to the presence of magnetic field distortion in the room—future work could choose a site which had no interference with the Earth's magnetic field in order to obtain a more accurate measurement. We also obtained 1.49 ± 0.01 for the ratio of the Landé g factors for the ground states of Rb^{87} and Rb^{85}, which compares well to the theoretical value of 1.5. For the values of the magnitudes of the Landé g factors, we obtain $g_f(Rb^{87}) = .520 \pm .001$ and $g_f(Rb^{85}) = .319 \pm .001$, while the theoretical values are $g_f(Rb^{85}) = \frac{1}{3}$ and $g_f(Rb^{87}) = \frac{1}{2}$. The actual values do not agree as well as the ratio, even with error bars, suggesting that there is some unaccounted-for systematic error which is not simple, as one value of the g factor is too large, and the other value is too small. One possibility may be that the field created by the Helmholtz coils is not perfectly uniform, as we assumed it to be, or that the Rb cell is not perfectly located at the center of the coils, which is where the equation for the magnetic field created by the Helmholtz coils is valid. Future work could more closely examine the nature of the magnetic field produced by the Helmholtz coils.

[1] A. L. Bloom, Scientific American (1960).
[2] R. Bernheim, *Optical pumping; an introduction* (W. A. Benjamin, 1965).
[3] J. L. Staff, *Junior lab reader* (2005).
[4] D. J. Griffiths, *Introduction to Quantum Mechanics* (Pearson Prentice Hall, 2005), 2nd ed.
[5] R. Benumof, American Journal of Physics **33**, 151 (1965).